

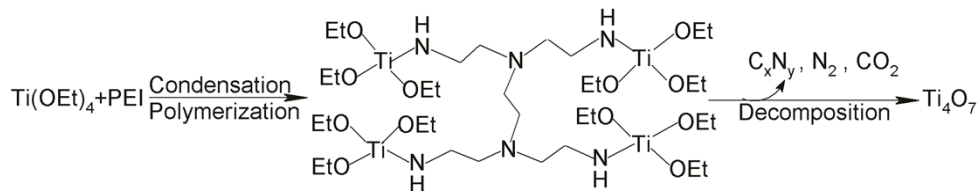
Supporting Information

A Metallic Oxide with High Electrochemical Activity for Aprotic Li-O₂ Batteries

Dipan Kundu, Robert Black, and Linda F. Nazar*

Experimental

Material preparation: In a typical synthesis, titanium(IV) ethoxide (Sigma Aldrich) and ethylenimine (oligomer mixture, $M_n \sim 400$, Sigma Aldrich) were mixed in a desired weight ratio. Ethanol/iso-propanol was added to control the viscosity of the obtained mixture, which was stirred at 75°C for overnight leading to the formation of an amber yellow color gel. The resultant gel was further dried at 100°C for 4 to 6 h, and then purged under Ar stream in a tubular flow furnace in a quartz tube for 3-4 h before firing at 860-870°C for 4 h with a heating ramp of 4°C/min. A possible reaction scheme is presented as follows:



Addition of ethylenimine to titanium ethoxide triggers a condensation reaction through coordination of the imine nitrogen to the Ti^{4+} of ethoxide, leading to the formation of three dimensional polymeric networks. Calcination under inert atmosphere results in the decomposition of the polymeric gel with concomitant release of carbon dioxide, nitrogen, and C_xN_y type gases along with the formation of nanoscopic TiO_2 in an amorphous carbon matrix. At higher calcination temperatures the carbothermal reduction of the TiO_2 begins with the release of CO_2 , resulting in the formation of porous Ti_4O_7 nanomaterial. The ethylenimine to titanium(IV) ethoxide ratio is controlled to generate almost carbon free crystalline phase of Ti_4O_7 .

Physical characterizations

XRD and Microscopy: Powder X-ray diffraction was carried out using a Bruker D8 advance diffractometer in Bragg-Brentano geometry with CuK_α ($\lambda = 1.5405 \text{ \AA}$) radiation. Scanning electron microscopy (SEM) was performed on a LEO 1530 field emission SEM. Transmission electron microscopy was carried out on a FEI Titan 80-300.

BET: Nitrogen adsorption-desorption analysis were performed at 77 K on a Quantachrome AUTOSORB-1. The sample was outgassed for 12 hours at 200°C under vacuum line prior to this analysis. The surface area of the sample was calculated by the Brunauer Emmett Teller (BET) method by taking at least 5 data points where $P/P_0 < 0.3$. Pore size distribution was obtained by the Barrett–Joyner–Halenda (BJH) method applied to the desorption branch of the isotherm.

Conductivity: Electrical conductivity of the Ti_4O_7 nanomaterial was measured on a 1.5 mm thick pellet of 12 mm in diameter, pressed with 4 ton pressure. The pellet was sintered at 400°C for 24 h under Ar flow. Electric conductivity was measured using a Jandel four-point probes connected with RM3000 test unit.

XPS: XPS analysis was performed on a Thermo ESCALAB 250 instrument configured with a monochromatic Al $\text{K}\alpha$ (1486.6 eV). The air-sensitive samples were transported to the spectrometer in an Ar atmosphere and transferred into the chamber very quickly. All spectra were fitted with Gaussian-Lorentzian functions and a Shirley-type background using CasaXPS software. For the analysis of Ti 2p spectra, three constraints were used on the fitting for component pairs: peak area ratio of 1:2 for $2p_{3/2}$: $2p_{1/2}$ and maximum 0.2 eV difference in full width half maximum (FWHM) with $2p_{1/2}$ having the higher value of FWHM. The binding energy values were all calibrated using the adventitious C 1S peak at 284.8 eV.

Electrochemistry: Tetraethylene glycol dimethyl ether (TEGDME, Sigma Aldrich, >99%) was distilled over Na metal under vacuum and stored over activated 4 Å molecular sieves in an Ar filled glove box. Lithium- bis(trifluoromethylsulfonyl)imide (LiTFSI, Solvionic, 99%) was dried at 120°C for 4 days under vacuum which was then used to obtain desired electrolyte, 0.5 M LiTFSI in TEGDME. The water content of the electrolyte was found to be < 1 ppm (Karl-Fischer titration).

Electrochemical performance was assessed using a hermetically sealed Swagelok type cell with the cathode head space filled with dry O₂ (<0.5 ppm) at 1.5 atm. For cathode fabrication, an ink obtained by blending Ti₄O₇ nanomaterial with PTFE suspension was coated on stainless steel mesh (mesh size: 100 x 100, 30% open area) of 1 cm² geometric area. The cathodes were then dried at 60°C for 1 h in air followed by 12 h at 300°C under dynamic vacuum. Typical loading of the electrodes were 3-5 mg cm⁻² with Ti₄O₇ to PTFE weight ratio of 90:10. Electrochemical cells were assembled in an Ar filled glove-box (O₂ < 0.5 ppm, H₂O < 0.5 ppm) using the 1 cm² cathode coins with Li metal foil as the anode and glass fiber (Millipore, 0.7 mm) as the separator (one). Glass fiber separators were dried at 300°C for 24 h under dynamic vacuum prior to use.

For the ex-situ analysis of the discharged and charged cathodes, cells were disassembled in an Ar filled glove-box and the electrodes were washed with dry acetonitrile (<1 ppm) and dried in a vacuum chamber. Galvanostatic cycling was performed using a BT2000 battery cycler (Arbin Instruments). All the current densities reported in this work are based on the geometric electrode area.

Mass Spectrometry: The residual gas analysis was performed with a modified design based on an OEMS apparatus reported by Tsiouvaras et. al (*J. Electrochem. Soc.* 160, p. A471-A477, 2013). A commercial electrochemical flow cell (EL-Cell, ECC-DEMS) is attached in-line with a gas flow controller (Bronkhurst, F-200CV) and quadrupole mass spectrometer (Standford Research Systems, RGA 200). During cell operation a controlled flow of Ar (5.0 Grade) sweeps the evolved gases from the cell to the MS entrance chamber where the gas enters the quadrupole through a fused silica capillary (50 um ID). The pressure inside the MS chamber is 2×10^{-6} torr during operation. Prior to measurement, the mass spectrometer is calibrated to establish a relationship between the measured ion current (A) and target gas concentration (ppm). With the use of known gas concentrations (from 2000 ppm O₂/Ar balance and 2000 ppm CO₂/Ar balance mixtures) mixed with different amounts of Ar, a linear relationship between the gas concentration and ion current is established. The quantification is performed with the use of Mathworks Matlab software.

For the measurements in Figure 2c and Figure 2d, cathodes were prepared in a 95:5 weight percent of active material : PTFE. The contents were spread onto a stainless steel mesh (2 cm²/100 mesh size) and dried under vacuum at 300 °C for 12 hours. The cells were assembled with 200 uL of 0.5M LiTFSI/TEGDME, two glass fiber separators and lithium metal as the

counter electrode. Discharge was performed at $250 \mu\text{A cm}^{-2}$ for the carbon cathode and $75 \mu\text{A cm}^{-2}$ for the Ti_4O_7 cathode under 1.5 atm O_2 to a fixed capacity of 1 mAh. *These values were chosen in order to provide suitable capacity for both cells, and a similar Li_2O_2 morphology (thin toroids in both cases).* Charging of the cell was performed at $250 \mu\text{A cm}^{-2}$ after a 2 hour rest period at OCV. Determination of the e^-/O_2 values was determined from the total accumulated amount of O_2 corresponding to voltages where O_2 evolution terminated (4.2 V for Ti_4O_7 and 4.5 V for VC).

For the online electrochemical mass spectrometry of the preloaded Ti_4O_7 cathode, commercial Li_2O_2 (Sigma Aldrich, 95% purity) was mixed with nano- Ti_4O_7 and PTFE suspension in isopropanol and the resultant slurry was coated on stainless steel mesh. The final composition of the cathode was $\text{Ti}_4\text{O}_7:\text{Li}_2\text{O}_2:\text{PTFE}::8:1:2$. The cathode was dried under vacuum overnight. The mass spectrometry cell was assembled in a similar way as described above. The cell was galvanostatically charged at a current density of $75 \mu\text{A cm}^{-2}$.

Estimation of Commercial Li_2O_2 Purity: Chemical purity of the commercial Li_2O_2 (Sigma Aldrich) was assessed by iodometric titration. The iodometric titration protocol is based on oxidation of a weighed quantity of peroxide with large excess iodide solution, followed by titration of the liberated iodine with standardized thiosulfate solution. Details of this protocol have been described elsewhere.¹ Commercial peroxide was found to be 88% pure by this titration method, and this was used to determine the actual mass of peroxide in the preloaded cathodes.

Table S1. Refined Lattice Parameters for Synthesized Nano-Ti₄O₇

Diffractometer:	Bruker D8 advance
Radiation	Cu K α
2 θ range	15-70
Step size	0.0085
Sec/step	4
Background	Chebyshev Polynomial
Chemical formula	Ti ₄ O ₇
Space group	A-1
a (Å)	5.6115(6)
b (Å)	7.1336(6)
c (Å)	12.521(2)
α (°)	94.9759(8)
β (°)	95.2475(7)
γ (°)	108.839(6)
Cell Volume (Å ³)	468.758(9)
Crystallite Size (nm)	16.33(1)
R _{exp}	1.246
R _p [%]	1.87
R _{wp} [%]	2.42
χ^2	1.94

*Determined by Rietveld refinement of the XRD data

Refined Lattice Parameters for Bulk Ti₄O₇ (for comparison)²

a (Å)	5.593(1)
b (Å)	7.125(1)
c (Å)	12.456(3)
α (°)	95.02(1)
β (°)	95.21(1)
γ (°)	108.73(1)

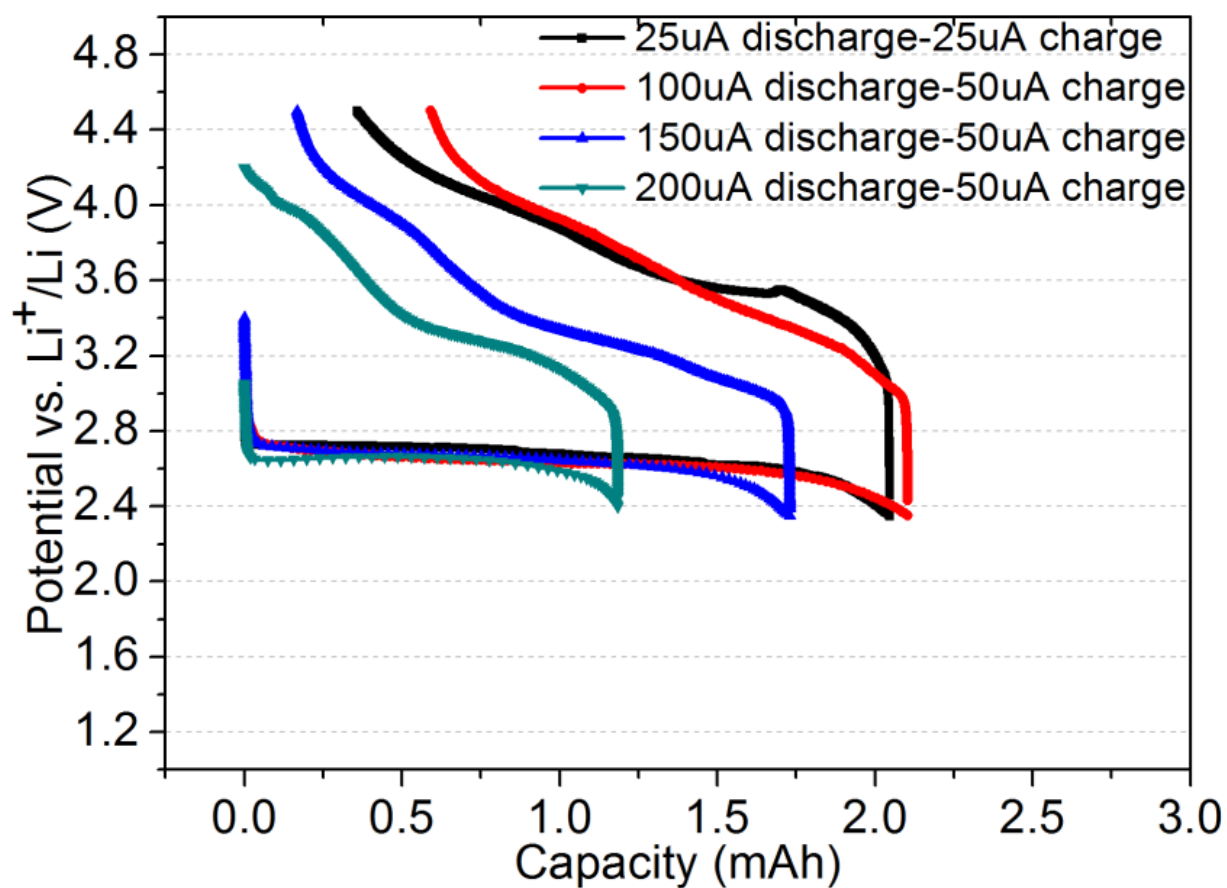


Figure S1. Galvanostatic cycling of the Ti_4O_7 cathode at different current densities. Inset description states the discharge and charge current densities applied to obtain the different discharge-charge profiles.

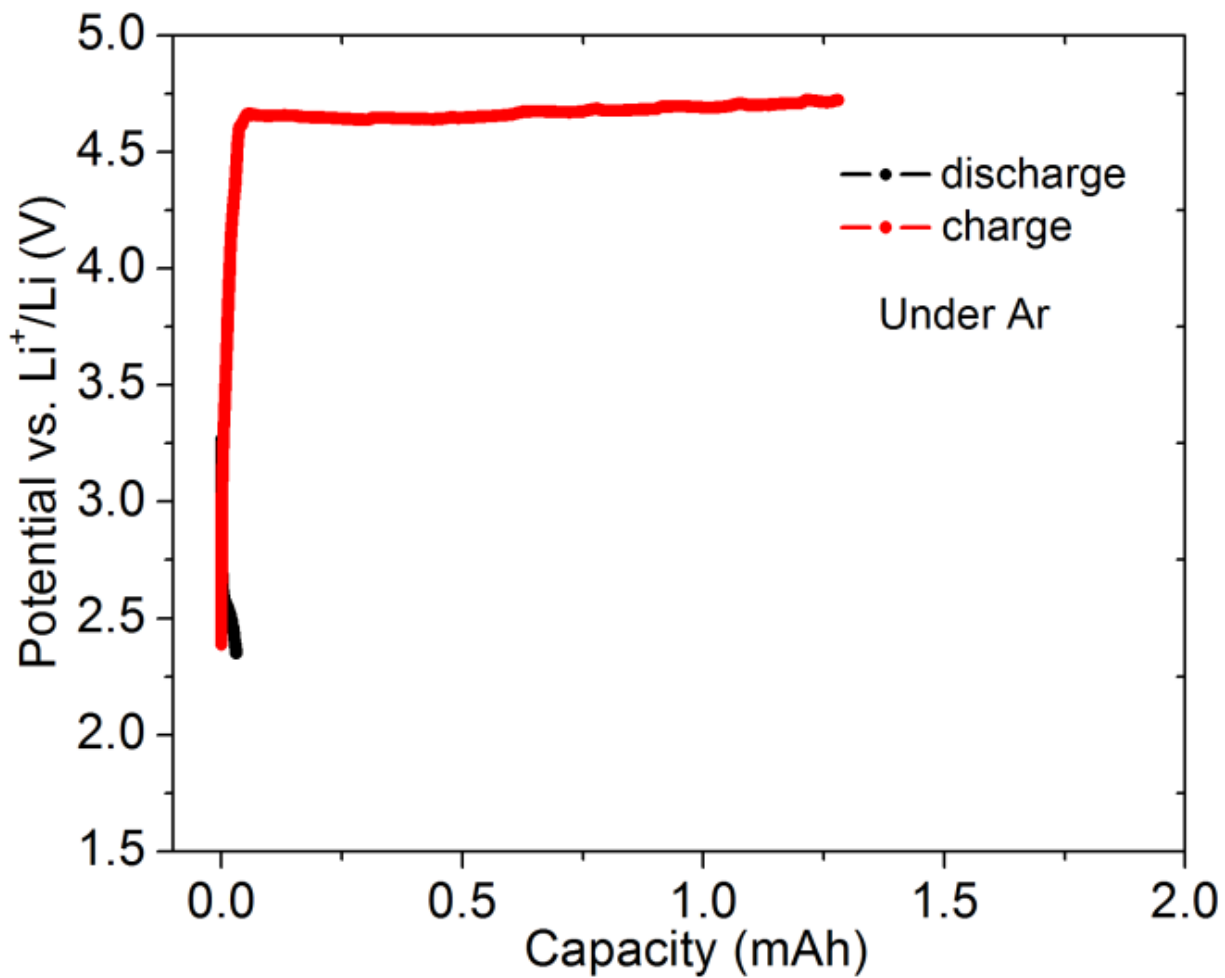


Figure S2. Galvanostatic discharge and charging profile of the Ti_4O_7 cathode in 0.5 M LiTFSI-TEGDME electrolyte under Ar between a voltage window of 2.3-4.7V vs. Li^+/Li .

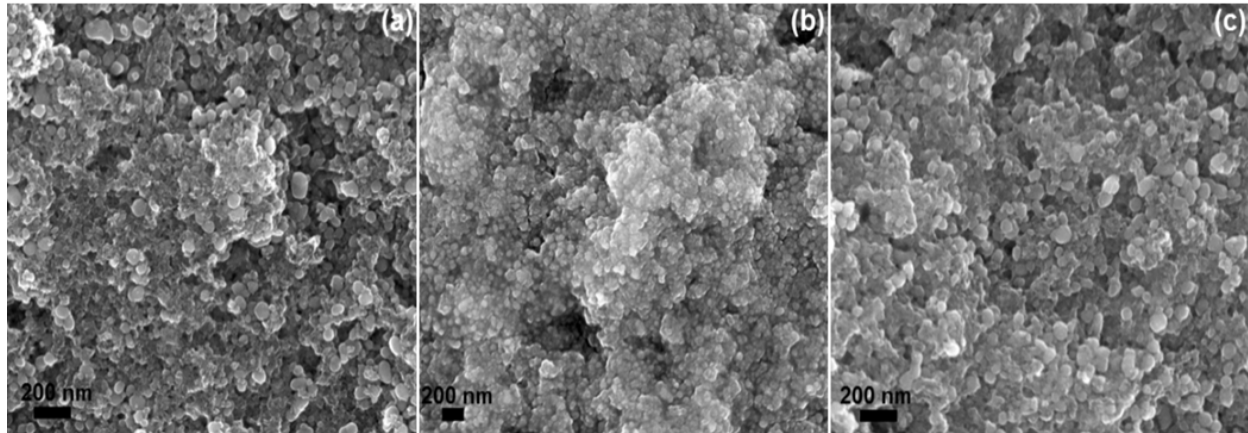


Figure S3. Ex-situ SEM investigations of the Ti_4O_7 cathode after electrochemical discharge and charge in a Li-O_2 cell. (a) SEM image of a pristine cathode showing its porous architecture; (b) cathode discharged at 200 uA cm^{-2} , illustrating the formation of the film-like Li_2O_2 that fills the inter-particle pores of the cathode; (c) cathode after electrochemical charging showing the removal of the Li_2O_2 .

Table S2. Comparison of the effect of current density on the Li_2O_2 morphology formed on Ti_4O_7 and VC cathode in a Li-O_2 cell, in 0.5 M LiTFSI-TEGDME electrolyte. Based on the BET surface area of Ti_4O_7 and VC, total available surface area on a 1 cm^2 cathode has been calculated assuming an average loading of 5 mg and 1 mg of Ti_4O_7 and VC, respectively. Here, $I_{\text{Geometric}}$ is the applied current density based on geometric surface area, and I_{Real} stands for current density expressed on total available surface area per 1 cm^2 cathode. The morphology of Li_2O_2 formed on a VC cathode has been discussed previously by our group.³

	Average Loading/cathode (g)	Geometric surface area/cathode (m^2)	BET surface area (m^2/g)	Total surface area/cathode (m^2)	Geometric current density ($\mu\text{A}/\text{cm}^2$)/Real current density/Morphology					
Ti4O7	0.005	10^{-4}	180	0.9	$I_{\text{Geometric}}$	25 $\mu\text{A}/\text{cm}^2$	50 $\mu\text{A}/\text{cm}^2$	100-150 $\mu\text{A}/\text{cm}^2$	200 $\mu\text{A}/\text{cm}^2$	
					I_{Real}	28 $\mu\text{A}/\text{m}^2$	56 $\mu\text{A}/\text{m}^2$	111-166 $\mu\text{A}/\text{m}^2$	222 $\mu\text{A}/\text{m}^2$	
					Morphology	Large toroids	Thinner toroids	Discs/platelets	Film	
Vulcan Carbon	0.001	10^{-4}	219	0.219	$I_{\text{Geometric}}$	5 $\mu\text{A}/\text{cm}^2$	10 $\mu\text{A}/\text{cm}^2$	25 $\mu\text{A}/\text{cm}^2$	50 $\mu\text{A}/\text{cm}^2$	
					I_{Real}	23 $\mu\text{A}/\text{m}^2$	46 $\mu\text{A}/\text{m}^2$	114 $\mu\text{A}/\text{m}^2$	228 $\mu\text{A}/\text{m}^2$	
					Morphology	Large toroids	Thinner toroids	Discs	Film	

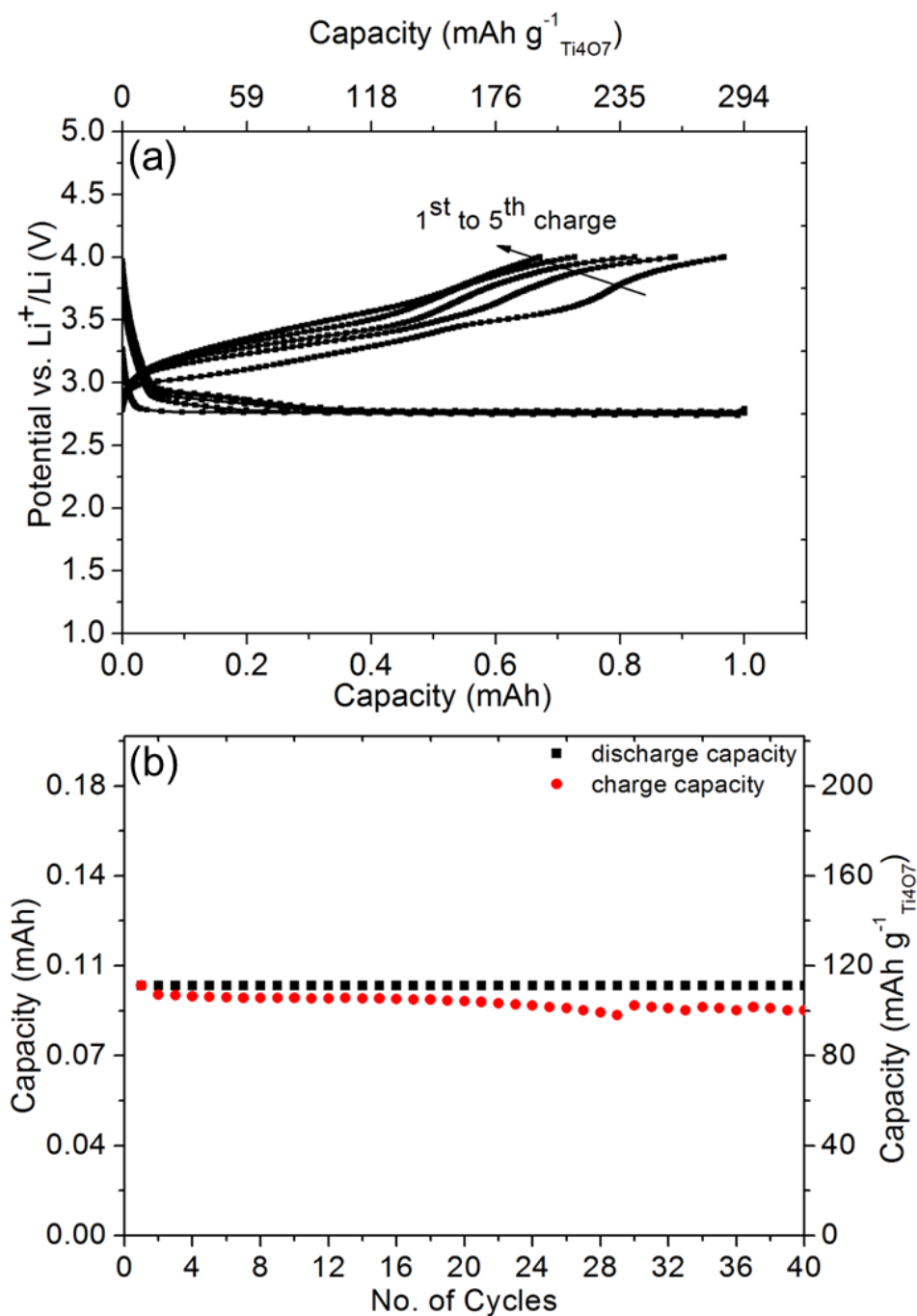


Figure S4. (a) galvanostatic cycling of the Ti_4O_7 cathode in a Li-O_2 cell with a capacity cutoff of 1 mAh in a 2.4-4 V voltage window against Li. 200 uA cm^{-2} of current density was applied for both discharge and charge. (b) galvanostatic cyclability of a Li-O_2 cell employing Ti_4O_7 cathode with a 0.1 mAh/ $\sim 100 \text{ mAh g}^{-1}$ capacity cutoff, cycled at 500 uA cm^{-2} current density. The cathode loading was adjusted to around 1 mg cm^{-2} to sustain a high current density.

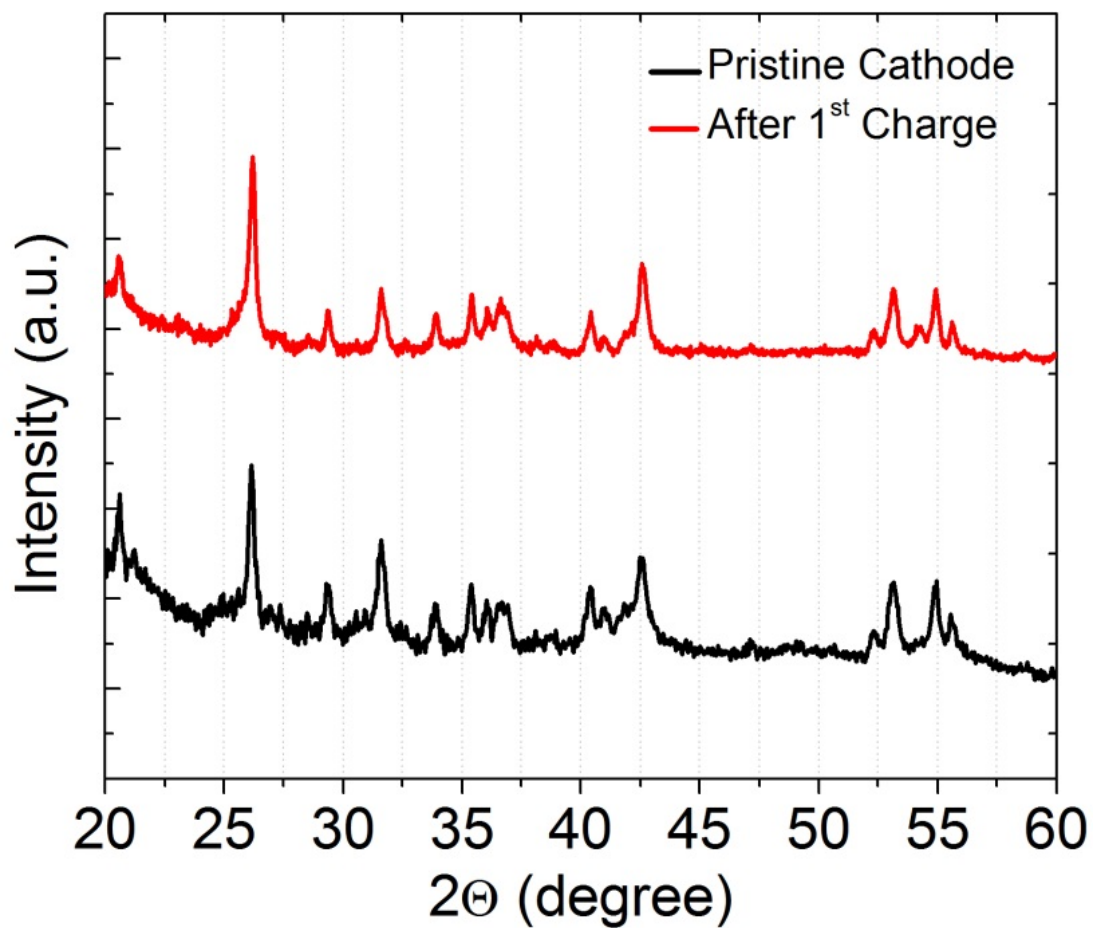


Figure S5. X-ray diffraction patterns of the pristine and a discharged/charged Ti₄O₇ cathode. The unchanged XRD pattern after electrochemical cycling demonstrates the chemical inertness of the bulk Ti₄O₇ in a Li-O₂ cell.

References:

1. B. D. McCloskey, A. Valery, A. C. Luntz, S. R. Gowda, G. M. Wallraff, J. M. Garcia, T. Mori and L. E. Krupp, *J. Phys. Chem. Lett.*, 2013, **4**, 2989-2993.
2. M. Marezio, D. B. McWhan, P. D. Dernier and J. P. Remeika, *J. Solid State Chem.*, 1973, **6**, 213-221.
3. B. D. Adams, C. Radtke, R. Black, M. L. Trudeau, K. Zaghbi and L. F. Nazar, *Energy Environ. Sci.*, 2013, **6**, 1772-1778.